Bubble nucleation in hydraulic systems

Alexander Terwort*, Tim F. Groß* and Peter F. Pelz*

Technische Universität Darmstadt, Chair of Fluid Systems, Otto-Berndt Straße 2, D-64287 Darmstadt, Germany*
E-Mail: Peter.Pelz@fst.tu-darmstadt.de

Free gas in a hydraulic system is usually accompanied by negative aspects. Currently available models usually underestimate degassing at liquid-gas interfaces that are exposed to fluid flows, which is the most relevant degassing mechanism in hydraulic systems. Therefore, a new approach for physical modelling of bubble formation at liquid-gas interfaces is presented. Based on recent findings on diffusion-driven nucleation a simple model to calculate the mass fraction of gas being set free in a hydraulic fluid is derived. This approach is experimentally validated and could be implemented in available calculation tools.

Keywords: Cavitation, oil hydraulics, degassing, diffusion-driven nucleation
Target audience: Mobile Hydraulics, Plant Design, Numerical Simulation

1 Introduction

The formation of gas bubbles in hydraulic fluids is usually accompanied by negative aspects. Dispersed gas opposes the secure and efficient operation of hydraulic machines. Some possible consequences of dissolved gas in hydraulic systems are a higher compliance, speed up of oil ageing, cavitation and deterioration of heat flux /3/. As the hydraulic fluid is an essential and often underestimated machine element, it is an engineer's task to make this element calculable.

Degassing is mainly driven by three different mechanisms:

1. permeability of connecting elements,
2. inclusion of air during assembly, and
3. degassing of the working liquid.

By using construction guidelines and norms developers, facility designers and users are able to reduce negative aspects /3/. While the first two mechanisms can be traced back to incorrect assembly or faulty constructions, degassing is a physical effect which cannot be avoided. Thus, degassing needs to be considered in an early design phase of components and facilities. Faulty design due to insufficient modelling of degassing processes in numerical simulations are usually linked to time- and cost-intensive iteration loops in the development processes. The advantage of numerical simulations becomes a disadvantage due to the insufficient quality of the results /21/.

In order to predict the dynamic performance of the hydraulic system calculation methods are necessary. Currently available models describing degassing processes in hydraulic systems are based on 0D-modelling. They include empirically determined parameters, which need to be calibrated for each use case /6, 25, 27/. These models are state of the art and widely used in the industrial context, even though they do not take degassing processes into account. Aside from 0D-modelling the application of commercial solvers (CFD) including cavitation models is possible. Yet, they do not provide validated models describing the degassing process /21/.

1.1 Preconditions for cavitation and degassing

Cavitation occurs when the pressure falls below a critical pressure, called Blake's threshold pressure /1/. Blake's threshold pressure is derived from a stability analysis of a spherical gas bubble. This bubble is called a nucleus. The analysis leads to an eigenvalue problem and finally Blake's threshold pressure, cf. /19,24/. The derived pressure is always lower than the vapour pressure of the fluid. Concluding from this, fluids are able to absorb tensile stresses. Thus, the necessary requirements for cavitation to occur are a pressure level below the critical pressure and the presence of a nucleus, cf. Figure 1.

In a degassing process the critical pressure is the saturation pressure of the fluid. If the local pressure is decreased below the saturation pressure, the local concentration c of dissolved gas is higher than the gas concentration in an equilibrium. The fluid is supersaturated. Based on Henry's law

$$c_s = p\,\mathcal{H} \tag{1}$$

with the pressure in the fluid p and the Henry coefficient $\mathcal{H}$, one can conclude that degassing processes only occur when the supersaturation of the fluid

$$\zeta := \frac{c}{c_s} - 1 \tag{2}$$

is greater than zero. Thus, $\zeta > 0$ is a necessary condition for degassing. As for the sufficient conditions, there are two possibilities. First, a sufficient supersaturation to form free bubbles in the liquid from the metastable phase due to the movement of gas molecules, which is called homogeneous nucleation theory, cf. /16/. Usually this theory is of minor importance in technical applications, as the necessary supersaturation of $\zeta \gg 100$ can not be reached. The second possibility is the existence of a liquid-gas interface which enables molecular mass transport. This has been investigated at TU Darmstadt in the last years. In this case the entrapment of gas in minor crevices, so-called surface nuclei, is of importance /8-13, 20/.

It is important to note that, in contrast to cavitation, vapour pressure is of minor relevance for degassing processes. There are attempts to include both degassing and cavitation in a unified theory /4, 14/. Yet, there are doubts whether cavitation can be a real cause of degassing or whether it acts as a reinforcement. The time step limiting degassing is the diffusion rate. This also needs to be considered in the theory of Iben et al. /14/.

1.2 Diffusion-driven nucleation

The necessary condition for degassing is a supersaturated fluid and the presence of a liquid-gas interface. In hydraulic components there are usually no free (liquid) surfaces, so the degassing potential is low. Yet, nuclei within the liquid and gas entrapped on surfaces cannot be avoided in technical applications. This is where degassing takes place. The nuclei contribute to the process in different ways. Dispersed gas bubbles and free floating particles are carried by the fluid, so they reside only for a short period of time in the locally supersaturated section. Hence, the amount of gas which can diffuse into the nucleus is limited. The degassing potential depends on the number of nuclei and their specific surface.

Consequently, degassing processes can be mainly observed at gas cavities in the walls limiting the flow, cf. figures 1 and 2. Gas cavities in cavities and cracks or attached to surface roughness elements, steps or drill holes serve as surface nuclei and allow the diffusion of gas that is solved in the liquid. The surface nuclei grow and free bubbles detach when a critical size is reached, cf. figure 1. The critical size depends on the geometry of the corresponding surface nucleus. The bubble detachment triggers the self-exciting process. In technical applications "new" supersaturated fluid constantly streams along the surface nuclei, so the process continues for a long time – in fact as long as the liquid is supersaturated. Only when the flow comes to rest, e.g. after turning off the hydraulic machine, an equilibrium will be reached and the degassing stops.

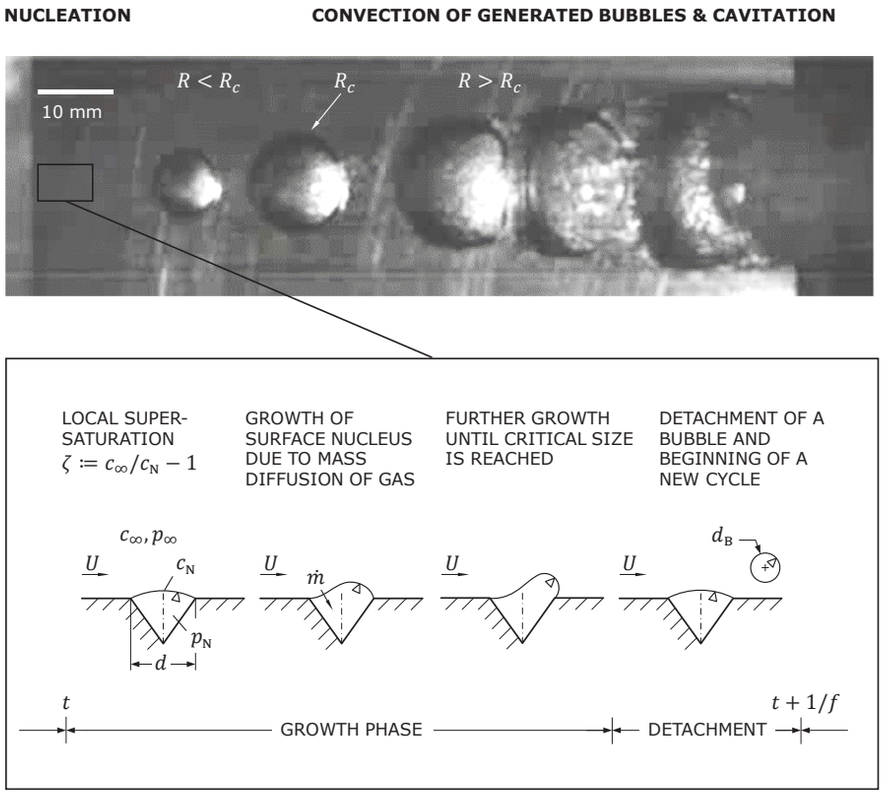

Figure 1: Nucleation by diffusion is a necessary condition for cavitation, cf. /10/. In this picture the flow goes from left to the right. Near the edge there is a nucleation site, which periodically detaches gas bubbles (no vaporization). The bubbles are carried into regions of lower pressure. If the pressure is decreased below Blake's threshold pressure the bubble becomes unstable. Resulting, the bubble strongly grows and rapidly collapses. This is the actual cavitation process. Contradicting common knowledge vaporization only plays a minor role. The sketch shows the diffusion-driven nucleation. As Groß and Pelz show, this is a self-exciting process /11/. Adapted from /7/.

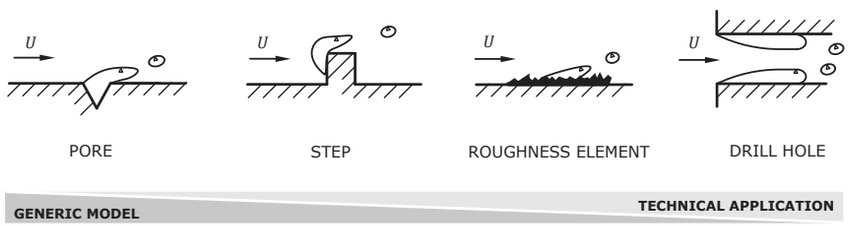

Figure 2: Boundary layers in pores, steps, roughness elements or in drill holes serve as nucleation sites and enable molecular mass flux and the generation of gas bubbles. Adapted from /7/.

The diffusion mass flux of solved gas into the surface nuclei and the following detachment of free gas bubbles is called diffusion-driven nucleation. It represents the most important mechanism of degassing in technical applications. The surface of the "produced" gas bubbles serve as additional liquid-gas interfaces. Free bubbles may also attach to roughness elements or steps and thus can act as surface nuclei. Thus, a large amount of gas can be set free. Figure 2 shows typical nucleation sites one can find in technical applications (drill holes, roughness elements) and their corresponding generic model (surface nuclei, steps).

There are only few scientific articles that focus on the degassing processes in technical flows. Bubble growth and detachment has been mainly investigated in quiescent liquids, cf. /15-17/. Yet, in technical applications the impact of the flow area on the mass flux and bubble detachment needs to be taken into consideration. Therefore, Peters and Honza /22/ created an experiment which allowed the investigation of nucleation in crevices. Blind holes with an inner diameter of 0.6 mm and 0.8 mm serve as nucleation sites. The authors found out that the nucleation rate, i.e. the frequency of bubble detachment, depends on the shear rate at the wall. Yet, they did not formulate a functional dependency. Nucleation rates of 1 Hz to 10 Hz were measured. Groß and Pelz enhanced the experimental setup from Peters and Honza to investigate nucleation and bubble detachment in more detail. They managed to reach nucleation rates of up to 1000 Hz in silicon oil, cf. /8-10/.

2 Modelling of degassing processes in technical fluids

In most cases it is argued that diffusion processes are too slow to have an impact on cavitation phenomena. This holds true for the bubble collapse. During bubble formation, diffusion-driven processes have to be taken into consideration, as Groß and Pelz showed /11, 20/. In this paper a new approach to estimate the molecular mass transport being set free in a fluid in motion is presented, cf. /7/.

Fick's first law of diffusion states that the mass flux of gas being dissolved in a liquid and transported across the phase boundary layer is given by

$$\dot{m} = -MD \int_A \nabla c \cdot \vec{n} dA, \tag{3}$$

where M is the molecular mass of the gas, D the diffusion coefficient, c the concentration of the gas solved in the liquid and $\vec{n}$ the vector normal to the surface A. Hence, the mass flux is proportional to the concentration gradient at the boundary layer. In order to obtain a high mass flux there needs to be either a large surface area or a high concentration gradient on the boundary layer. Since the concentration gradient cannot be measured directly, its extent is probably underestimated in most cases, leading to the misjudgement of diffusion processes as described before.

The concentration field in the liquid satisfies the advection diffusion equation

$$\frac{\partial c}{\partial t} + \vec{u} \cdot \nabla c = \nabla \cdot (D \nabla c), \tag{4}$$

which yields the concentration gradient. Figure 3 shows two common configurations for degassing in hydraulic systems. The concentration of dissolved gas in the liquid is c_∞. The concentration determined by the local pressure at the liquid-gas interface is c_N. Hence, the supersaturation can be calculated with equation (2).

On the left side of figure 3 a surface nucleus with an inner diameter d is shown. In this case the diameter is the characteristic length. If the surface nuclei are much smaller than the length of the components (pipe diameter, gap height) the velocity field $u(y)$ can be linearized near the wall, $u(y) = \dot{\gamma} y$, with wall shear rate $\dot{\gamma}$. This approximation is also valid for turbulent flows, if the concentration boundary layer lies within the viscous sublayer of the flow. Usually the concentration boundary layer is much smaller than the boundary layer of the flow, so the condition is usually satisfied (high Schmidt-Numbers $Sc := \nu / D \gtrsim 10^3$).

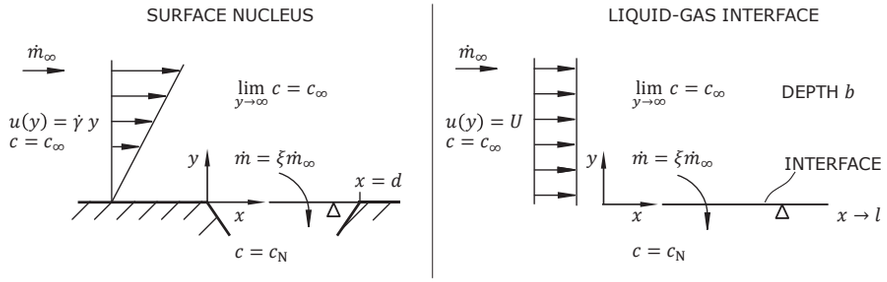

Figure 3: Principal sketch of the present advection-diffusion problem. Left: Surface nucleus with shear flow. Right: Liquid-gas interface with homogenous flow profile. Adapted from /7/.

On the right side of figure 3 a liquid-gas interface with a homogeneous flow is shown. This configuration represents the case of a bubble attached to a step or surface roughness element, cf. figure 2. Here *l* is the characteristic length describing the size of the liquid-gas interface. The depth of the problem is *b*.

For stationary processes, a constant diffusion coefficient *D*, a flow velocity *u(y)* parallel to the surface with $\vec{n} = \vec{e}_y$ and a negligible diffusion in the direction of the flow equation (4) can be written as

$$u(y)\frac{\partial c}{\partial x} = D\frac{\partial^2 c}{\partial y^2}. \tag{5}$$

For the problems sketched in figure 2 boundary layer theory provides the solutions presented in table 1, cf. /10, 17/.

Table 1: Solution of the boundary layer equation (5) for the configurations sketched in figure 2.

	Velocity Field	Dimensionless Number	Solution of Eq. (5)	
Surface Nucleus with shear flow	$u(y) = \dot{\gamma} y$	$Pe = \frac{\dot{\gamma} d^2}{\mathcal{D}}, Sh = \frac{\dot{m}}{c_N \zeta M \mathcal{D} d}$	$Sh = 0.66\, Pe^{1/3}$	(6)
Boundary Layer with homogeneous flow	$u(y) = U$	$Pe = \frac{Ul}{\mathcal{D}}, Sh = \frac{\dot{m}}{c_N \zeta M \mathcal{D} b}$	$Sh = \frac{2}{\sqrt{\pi}}\, Pe^{1/2}$	(7)

As the solutions show the problem can be described by the dimensionless Péclet-Number *Pe* and the Sherwood-Number *Sh*. The Sherwood-Number corresponds to a dimensionless mass flux, while the Péclet-Number describes the ratio of advective flows and diffusive flows. The higher the Péclet-Number, the thinner the concentration boundary layer. Thin concentration boundary layers lead to high concentration gradients and, thus, high mass flux. The exponents 1/2 and 1/3 result from different velocity fields.

2.1 Derivation of a degassing model for oil hydraulics

The results of the degassing mass flux can be used in two different ways. On the one hand, the mass flux can be used to determine the size and amount of bubbles detaching from the boundary layer. This is of special interest in the case of hydrodynamic cavitation and has been discussed by Groß and Pelz in /11, 20/, cf. figure 1.

For the development and design of hydraulic systems this detailed knowledge is not required most of the time, as the current 0D-modelling indicates, cf. /21/. For hydraulic applications integral parameters like the diffusion mass flux $\dot{m}$, the mass flux ratio $\xi = \dot{m}/\dot{m}_\infty$ and the volume flow ratio φ are much more important, cf. /13/. The mass flux of the dissolved gas in the liquid can be determined by

$$\dot{m}_\infty = Q\, c_\infty M = Q\, p_s\, \mathcal{H}\, M. \tag{8}$$

Q represents the flow rate, p_s the saturation pressure of the liquid and c_∞ the concentration of the dissolved gas in the liquid. The ratio ξ describes the mass fraction of the dissolved gas being set free while flowing through the respective component. The volume fraction can be determined from the mass fraction. It depends on the local pressure p_∞ and the saturation pressure p_s. The volume fraction characterizes the amount of air in relation to the volume of the liquid and is given by

$$\varphi = \xi\, \Lambda\, \frac{p_s}{p_\infty}. \tag{9}$$

Here $\Lambda := \mathcal{R}\, T\, \mathcal{H}$ is the dimensionless solubility (= Ostwald coefficient) with the universal gas constant $\mathcal{R}$ and the temperature *T*. In the following the solutions for a boundary layer overflown by a homogeneous velocity field is used, cf. equation (7). The solution is an upper boundary of the degassing mass flux. The considered boundary layer has the length *l* and the depth *b*.

The degassing max flux

$$\dot{m} = \frac{2}{\sqrt{\pi}} c_N \zeta M D b \left(\frac{Ul}{D}\right)^{1/2} = \frac{2}{\sqrt{\pi}} c_N \zeta M D b\, Pe^{1/2} \tag{10}$$

yields the mass flux ratio

$$\xi := \frac{2}{\sqrt{\pi}} \frac{\zeta}{\zeta + 1} \left(\frac{U D b^2 l}{Q^2}\right)^{1/2} = \frac{2}{\sqrt{\pi}} \frac{\zeta}{\zeta + 1} \frac{Db}{Q} Pe^{1/2} \tag{11}$$

and the volume flux ratio

$$\varphi := \frac{2}{\sqrt{\pi}} \zeta \Lambda \left(\frac{U D b^2 l}{Q^2}\right)^{1/2} = \frac{2}{\sqrt{\pi}} \zeta \Lambda \frac{Db}{Q} Pe^{1/2}. \tag{12}$$

Mass fraction and volume fraction increase with increasing supersaturation ζ and flow velocity *U*. An increasing volume flux decreases both parameters. Usually there is a functional dependency between the flow velocity near the liquid-gas interface U_∞ and the volume flux *Q*.

If *b* is the circumference of a circular flow cross section (e.g. a pipe or nozzle), so the whole circumference surface is coated by a liquid-gas interface, the volume flux is given by $Q = Ub^2/(4\,\pi)$.

Inserted in equations (11) and (12) yields

$$\xi = 8\sqrt{\pi}\, \frac{\zeta}{\zeta + 1} \frac{l}{b} \left(\frac{D}{bl}\right)^{1/2} = 8\sqrt{\pi} \frac{\zeta}{\zeta + 1} \frac{l}{b} Pe^{-1/2} \tag{13}$$

and

$$\varphi = 8\sqrt{\pi}\zeta\Lambda \frac{l}{b} \left(\frac{D}{Ul}\right)^{1/2} = 8\sqrt{\pi}\, \zeta\Lambda \frac{l}{b} Pe^{-1/2}. \tag{14}$$

On first sight it may be remarkable, that mass fraction and volume fraction of the free gas decrease with increasing flow velocity, respectively Péclet-Number. For a constant volume flow $Q \propto U\, b^2$ the mass fraction and volume fraction only depend on the supersaturation ζ, the diffusion coefficient *D* and the characteristic length of the boundary layer *l*. Additionally, the volume fraction depends on the solubility Λ.

The supersaturation ζ itself is also a function of the flow velocity, as an increasing flow velocity decreases the local static pressure and consequently the local saturation concentration c_N. The ratio l/b in equation (14) can be

interpreted as ratio of the area bl, which is available for degassing, and the cross section of the flow, which is proportional to b^2. A high ratio l/b yields high mass- and volume fractions.

The model is based on the assumption of the concentration of dissolved gas in the liquid remaining constant. Therefore, for small Péclet-Numbers values of ξ and φ greater than one can be calculated. As most technical applications have high flow velocities, and therefore high Péclet-Numbers, there is no correction necessary. If the Péclet-Number is low, the decrease of dissolved gas in the liquid needs to be taken into consideration, leading to a differential equation of first order.

The derived correlations, equation (10)-(14), can provide important knowledge on the design of hydraulic components or systems. In contrast to the available, empirical 0D-models the flow velocity is taken into consideration. This is a necessary condition for most use cases. The determination of the size of the boundary layer is difficult in most cases. Yet the new approach is predominant to empirical parameters, as it is based on physically stable parameters. The approximation of the surface area being available for degassing enhances the understanding of the system, enables identification of critical components and inappropriate assembly positions and therefore contributes to the optimization of hydraulic components and systems. In the following the application of the model is demonstrated.

3 Application of the model

In this example a micro orifice with an inner diameter D = 0.2 mm and a length l = 2 mm is considered. These dimensions correspond to the orifice being experimentally investigated by Freudigmann et al. (cf. /4-5/). The fluid used in the experiments is Shell V-Oil 1404. An initial pressure of 60 bar leads to a mass flux of 2 g/s. The density is 826 kg/m^3. The fluid is saturated at atmospheric pressure and the solubility is $\Lambda = 0.12$. For simplification a homogeneous flow profile within the orifice is assumed. In this case the velocity is 77 m/s.

Using equation (13), $b = \pi D$ and the estimation of $c_N/c_\infty \to 0$, corresponding to $\zeta/(\zeta+1) \to 1$, a mass ratio of $\xi = 5 \times 10^{-3}$ is determined. Regarding experimental results, cf. /3/, this result seems feasible. The experiments of Freudigmann et al. show that degassing strongly depends on the pressure downstream of the orifice. A reduced pressure leads to a higher mass ratio. The measured mass ratios range from 10^{-3} at 4 bar and 10^{-1} at 2 bar. The increase of mass ratio can be at least partially explained by the increase of the surface area corresponding to the increase of the volume of dispersed gas (ideal gas law). Especially the gas being entrapped in vortexes behind the aperture plays an important role. Effects primarily affecting the development of the flow and not degassing are not taken into account.

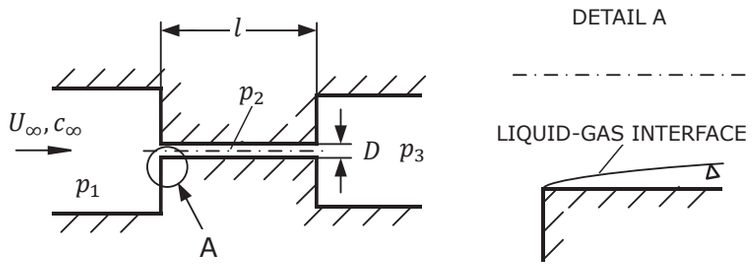

Figure 4: Application of the degassing model on a micro orifice flow. Adapted from /6/.

In future investigations the degassing model has to be validated with more experimental data. In addition to that, experimental investigations shall provide detailed predictions on the surface of the boundary layer. The long-term objective is to implement the model in available fluid solvers. To provide an example, the presented problem was implemented in the object-oriented modelling language Modelica. The source code is shown in figure 5. In contrast to common programming languages Modelica uses equations instead of assignments, enabling the user to describe and simulate complex physical systems more easily than in traditional programming languages. In this case, the existing model of a straight pipe with a rough surface was extended by adding the additional variables necessary to calculate the Péclet number Pe, oversaturation ζ and mass fraction ξ. Further properties of the pipe already known to the user, like the pipe diameter or its length, can be used without additional modelling. Finally, the subset of equations is introduced. In a typical application, the model is connected by its ports A and B with the connecting elements, for example a water reservoir or closed tank.

```
model DegassingOrifice "Straight Pipe with the ability to calculate the amount
of free gas in the liquid"
  // extend standard model StaticPipe
  extends Modelica.Fluid.Pipes.StaticPipe;

  // import SI units
  import SI = Modelica.SIunits;   // import SI units

  // Initialize model variables
  Real pi = Modelica.Constants.pi "Definition of pi as local variable";
  parameter Modelica.SIunits.DiffusionCoefficient D = 2e-9
    "Diffusion coefficient"
    annotation(Dialog(tab = "Initialization"));
  Modelica.SIunits.MassFraction xi "Mass fraction of gas";
  Real zeta "Oversaturation of the liquid";
  SI.PecletNumber Pe "Peclet Number";

equation
  // Mass of gas unsolving from the liquid
  Pe = D/(port_a.m_flow/(flowModel.rhos[1]*crossArea)*length);
  zeta = port_a.p/port_b.p -1;
  xi = 8*sqrt(pi)*(zeta/(zeta+1))*length/perimeter*Pe^0.5;

  annotation (defaultComponentName="Pipe", …));
end DegassingOrifice;
```

Figure 5: Modelica source code.

4 Conclusion

Degassing of fluids in technical systems is an important objective due to its extensive negative impacts on the efficient and secure operation of hydraulic components. Currently available modelling approaches enable the estimation of degassing in tanks but fail when it comes to formation of bubbles near boundary layers. The formation of bubbles near boundary layers between liquid and gas, so called nucleation sites, is the most common and therefore most relevant degassing mechanism in hydraulic systems.

The present paper presents new findings on degassing in hydraulic systems and highlights the relevance for technical applications. Based on the presented degassing model calculations of the mass flux ratio and volume flux ratio may be performed. Contrary to available 0D-models no empirical parameters are used. If the model is implemented by software developers, future design calculations may be performed in more detail. The application of the degassing model optimizes systems understanding and enables the development of optimized components and systems.

Nomenclature

Variable	*Description*	*Dimension*
A	Surface area of the boundary layer	L^2
b	Depth of the problem	L
c	Gas concentration of the fluid	L^3N^{-1}
c_N	Gas concentration at the boundary layer	L^3N^{-1}
c_S	Saturation concentration of the gas in the liquid	L^3N^{-1}
c_∞	Gas concentration in the surrounding fluid	L^3N^{-1}
D	Pipe diameter	L
$\mathcal{D}$	Diffusion coefficient	L^2T^{-1}
d	Diameter of the crevice	L
$\mathcal{H}$	Henry-Coefficient	$L^{-2}M^{-1}T^2N$
l	Characteristic length of the boundary layer	L
M	Molar mass	MN^{-1}
$\dot{m}$	Outgassing mass flux	MT^{-1}
$\dot{m}_\infty$	Mass flux of dissolved gas	MT^{-1}
N	Number of nuclei	1
$\vec{n}$	Normal vector	1
p	Pressure	$L^{-1}MT^{-2}$
p_S	Saturation pressure	$L^{-1}MT^{-2}$
p_∞	Pressure of the liquid	$L^{-1}MT^{-2}$
Q	Volume flux	M^3T^{-1}
$\mathcal{R}$	Universal gas constant	$L^2MT^{-2}N\Theta$
T	Temperature	Θ
T	Time	T
$\vec{u}$	Velocity field	LT^{-1}
U	Velocity homogenous flow	LT^{-1}
x	Coordinate	1
y	Coordinate	1
$\dot{\gamma}$	Shear rate at the wall	T^{-1}
ζ	Oversaturation	1
Λ	Gas solubility	1
ν	Viscosity of the liquid	L^2T^{-1}
ξ	Mass fraction	1
ϱ	Density of the liquid	$L^{-3}M$
φ	Volume fraction	1
Pe	Péclet Number	1
Sc	Schmidt Number	1
Sh	Sherwood Number	1

References

/1/ Blake, F.G., *The Onset of Cavitation in Liquids, Tech. Memo. No. 12*, Acoustics Res. Lab., Harvard University, 1949.

/2/ Brennen, C.E., *Cavitation and bubble Dynamics*, Oxford University Press, 1995.

/3/ Findeisen, D., *Ölhydraulik: Handbuch für hydrostatische Leistungsübertragung in der Fluidtechnik*, Springer, 5. Edition, 2006.

/4/ Freudigmann, H.-A., Iben, U., Pelz, P.F., *Air release measurements of V-oil 1404 downstream of a micro orifice at choked flow conditions*, Proceedings of 9th International Symposium on Cavitation (CAV2015), Lausanne, 2016.

/5/ Freudigmann, H.-A., Iben, U., Dörr, A., Pelz, P.F., *Modeling of Cavitation-Induced Air Release Phenomena in Micro-Orifice Flows*, In: J Fluids Eng, 139(11), 2017.

/6/ Furno, F., Blind, V., *Effects of air dissolution dynamics on the behaviour of positive-displacement vane pumps: a simulation approach*. Proceedings of the 10th International Fluid Power Conference, Dresden, 2016.

/7/ Groß, T.F., Ludwig, G., Pelz, P.F., *Axiomatisches Modell für die Bildung von freiem Gas in Hydrauliksystemen*, accepted in O+P – Ölhydraulik und Pneumatik, 2017.

/8/ Groß, T.F., Ludwig, G., Pelz, P.F., *High-Speed Visualisierung von Keimbildungsvorgängen an wandgebundenen Porenkeimen,* Lasermethoden in der Strömungsmesstechnik GALA e.V., Dresden, 2015.

/9/ Groß, T.F., Ludwig, G., Pelz, P.F., *Experimental evidence of nucleation from wall-bound nuclei in a laminar flow*, Proceedings of 9th International Symposium on Cavitation (CAV2015), Lausanne, 2015.

/10/ Groß, T.F., Ludwig, G., Pelz, P.F., *Experimental and theoretical investigation of nucleation from wall-bound nuclei in a laminar flow,* Proceedings of 16th International Symposium in Transport Phenomena and Dynamics of Rotating Machinery, Honolulu, 2016.

/11/ Groß, T.F., Pelz, P.F., *Diffusion-driven nucleation from surface nuclei in hydrodynamic cavitation*, In: J Fluid Mech 830, 138-164, 2017.

/12/ Groß, T.F., Bauer, J., Ludwig, G., Fernandez Rivas, D., Pelz, P.F., *Bubble nucleation from Micro Crevices in a Shear Flow*, In: Exp Fluids 59:12, 2018.

/13/ Groß, T.F., *Diffusionsgetriebene Keimbildung an Porenkeimen in kavitierenden Strömungen*, PhD-Thesis, TU Darmstadt, 2017.

/14/ Iben, U., Wolf, F., Freudigmann, H.-A., Fröhlich, J., Heller, W., *Optical measurements of gas bubbles in oil behind a cavitating micro-orifice flow,* In: Exp Fluids 56:114, 2015.

/15/ Jones, S.F., Evans, G.M., Galvin, K.P., *Bubble nucleation from gas cavities – a review,* In: Adv Colloid Interface Sci 80, 27-50, 1999.

/16/ Jones, S.F., Evans, G.M., Galvin K.M., *The cycle of bubble production from a gas cavity in a supersaturated solution*, In: Adv Colloid Interface Sci 80:51-84, 1999.

/17/ Liger-Belair, G., Marchal, R., Robillard, B., Dambrouck, T., Maujean, A., Vignes-Adler, M., Jeandet, P., *On the velocity of expanding spherical gas bubbles rising in line in supersaturated hydroalcoholic solutions: Application to bubble trains in carbonated beverages,* Langmuir 16(4), 2000.

/18/ Mersmann, A., *Stoffübertragung*, Springer-Verlag Berlin, 1986.

/19/ Pelz, P.F., *Cavitation*, Lecture Notes, Darmstadt, 2008.

/20/ Pelz, P.F., Keil, T., Groß, T.F., *The transition from sheet to cloud cavitation,* In: J Fluid Mech 817, 436-454, 2017.

/21/ Pelz, P.F., Groß, T.F., Ludwig, G., *Vergleichende Bewertung von Modellen für Kavitation und Ausgasung – ein Plädoyer für validierte Theorie als Voraussetzung für Zeit- und Kostenersparnis im Entwicklungsprozess,* submitted to O+P – Ölhydraulik und Pneumatik, 2017.

/22/ Peters, F., Honza, R., *A benchmark experiment on gas cavitation,* In: Exp Fluids 55:1786, 2014.

/23/ Schmitz, K., Kratschun, F.M., Murrenhoff, H., *Simulation der Dynamik einer Gasblase zur Untersuchung des Diesel-Effekts in hydraulischen Systemen*, O+P – Ölhydraulik und Pneumatik 5, 2016.

/24/ Spurk, H.J., *Aufgaben zur Strömungslehre*, Springer-Verlag Berlin, 1996.

/25/ Schrank, K, Stammen, C., Murrenhoff, H., *A new approach to model a multi-phase hydraulic capacity and its experimental validation,* Proceesings of 9th International Fluid Power Conference, Aachen, 2014.

/26/ van Wijngaarden, L., *Shock Waves in Bubbly Liquids,* Shock Wave Science and Technology Reference Library. Springer Berlin, 2007.

/27/ Zhou, J., Vacca, A., Manhartsgruber, B., *A novel approach for the prediction of dynamic features of air release and absorption in hydraulic oil,* In: J Fluids Eng 135(9), 2013.